

Unclassified

3-D Finite Element
Simulation of the PCCv
Specimen Statically Loaded
in Three-Point Bending
Convention Electrabel-SCK•CEN

M. Scibetta

RMR
SCK•CEN, Mol, Belgium

BLG-860 Revision 1

January 2001

DISTRIBUTION LIST

Author	SCK•CEN	1 copy
E. van Walle	SCK•CEN	1 copy
R. Chaouadi	SCK•CEN	1 copy
E. Lucon	SCK•CEN	1 copy
J.-L. Puzzollante	SCK•CEN	1 copy
R. Gérard	Tractebel	1 copies
Secretary RMO	SCK•CEN	5 copies

Total of 11 copies

This document has been written and approved by:

		Date	Approval
Author:	M. Scibetta		
Verified by:	R. Chaouadi		
Approved by:	E. van Walle		

3-D Finite Element Simulation of the PCCv
Specimen Statically Loaded in Three-Point Bending
Convention Electrabel-SCK•CEN

M. Scibetta

BLG-860 Revision 1

Contractnr: KNT 90 99 1165.01

RMR
SCK•CEN, Mol, Belgium

January 2001

FOREWORD

This revision was performed in order to take John Underwood's comments into account. Changes were done to:

- correct for a typo in equation (14),
- better explain the context in which John Underwood's equation was established,
- better set the limit of applicability of $r_p=0.44$

TABLE OF CONTENTS

1	Introduction.....	4
2	FE model.....	5
3	Finite element results	9
4	Discussion.....	15
	Conclusions.....	19
	Acknowledgements	20
	References	20

ABSTRACT

The objective of this work is to perform three-dimensional finite element calculations of a fracture toughness test in the transition region where fracture initiates through a cleavage mechanism. The selected geometry is the PCCv specimen statically loaded in three point bending with a crack length equal to the half of the width.

After a number of iterations, an appropriate mesh, boundary conditions and finite element model were selected.

Finite element calculations of the PCCv are used to analyse:

- the relation between the load point displacement and the crack mouth opening displacement,
- the η -factor formulation,
- the effect of side-grooving,

It is found that the different formulations proposed in the ASTM E1921-97 to calculate the J-integral are accurate enough for its application. The maximum error on the reference temperature is 3 °C.

The use of the plane strain Young modulus and adequate formulation to infer the load line displacement are presented and discussed.

KEYWORDS

Finite element calculations, three-dimension, PCCv, side-groove, fracture toughness, cleavage, CMOD, LLD, η -factor

1 Introduction

Fracture toughness testing in the transition regime was recently standardised within ASTM 1921-97 [1]. This standard proposes a normalised procedure to analyse the test results of standard specimens and to determine the reference temperature, T_0 , for ferritic steels in the transition range.

The assessment of Reactor Pressure Vessel Steel (RPVS) embrittlement could be usefully evaluated through the shift of the reference temperature ΔT_0 instead of the current semi-empirical methodology. In practice, standard one inch thickness Compact Tension, C(T), specimen can be usefully replaced with smaller fracture toughness specimens, such as the precracked Charpy v-notch Specimen (PCCv). Indeed, irradiated RPVS is available in small quantities and PCCv specimens can be reconstituted from broken surveillance Charpy specimen [2].

The published literature shows that the PCCv specimen analysed using the ASTM 1921 generally shows a 10 °C lower reference temperature than the standard specimen. Compared with the inherent scatter in the transition, this difference is small. However, it has been observed on many materials: JSPS [3, 4], 22NiMoCr37 [4], JRQ [4, 5], 73W [4], KFY5 [5] and JFL[5].

The reason for this difference can be:

- a non adequate formulation to derive the fracture toughness from the load displacement record,
- a different level of constraint in single edge notch bend SE(B) and C(T) geometry [3],
- a different level of constraint due to side-grooving,
- a different level of constraint due to the ratio W/B which is 1 for PCCv and 2 for C(T) [3],
- an inadequate size limit defined to avoid loss of constraint [3],
- a lower reference temperature for lower test temperature, as PCCv specimens are generally tested at lower temperatures to increase the number of valid data.

The formulation and the level of constraint can be investigated using finite element simulations of the PCCv and one inch C(T) fracture toughness test. However, simple 2-dimensional analysis of a PCCv specimen, assuming a plane strain behaviour, is not an adequate model to accurately describe the actual 3-dimensional geometry [6, 7].

The recommendations of the ASTM E1921-97 to derive the fracture toughness from the load versus displacement record and to use a size limit to avoid loss of constraint are partly based on the work of Nevalainen and Dodds [7]. They performed a thorough 3-dimensional finite element analysis of the C(T) and SE(B). They provide:

- η -factors that are to be used to experimentally evaluate the fracture toughness,
- specimen size limits accepting a limited loss of constraint (10% overestimated fracture toughness),
- an effective thickness introduced for the statistical correction, which takes into account triaxiality changes along the crack front.

It is important to note that the current ASTM E1921-97 specimen size requirement is less severe than the specimen size requirement established by Nevalainen and Dodds in [7]:

$$b, B > \frac{MK^2}{E\sigma_{YS}} \quad (1)$$

with $M=30$ for the ASTM E1921-97 and $M=55$ according to [7] for a strain hardening exponent $n=0.1$.

The application of equation (1) to a PCCv specimen with $b=5$ mm and $\sigma_{YS}=500$ MPa has for consequence that PCCv specimens that break between 96.5 and 130 MPa \sqrt{m} are subject to a significant loss of constraint. This loss of constraint is such that the fracture toughness might be overestimated by more than 10%. This overestimated fracture toughness might explain the lower reference temperature measured with small specimens. Indeed, 10% higher median fracture toughness corresponds to a 6 °C lower reference temperature.

In order to develop a loss of constraint correction factor for small specimens and to gain confidence in the results presented in [7], a study was performed at SCK•CEN. This work is done within Task 1.1.3 of the ELECTRABEL -SCK•CEN Convention. The first part of this study is to perform and analyse the finite element simulations of a fracture toughness test on a PCCv specimen. In a further step, the finite element calculation of a C(T) one-inch thickness specimen loaded up to 100 MPa \sqrt{m} will be required to obtain a reference condition.

2 FE model

To model actual material behaviour, the incremental theory of plasticity is used in combination with an isotropic strain-hardening model based on the Von Mises criterion with a uniaxial true stress versus true strain described by a power law:

$$\frac{\sigma}{\sigma_{YS}} = \begin{cases} \frac{\epsilon}{\epsilon_{YS}} & \text{if } \sigma < \sigma_{YS} \\ \left(\frac{\epsilon}{\epsilon_{YS}}\right)^n & \text{if } \sigma \geq \sigma_{YS} \end{cases} \quad (2)$$

$$\text{with } E \epsilon_{YS} = \sigma_{YS} \quad (3)$$

Actual true stress versus true strain behaviour of metallic materials can generally be fitted by a power law curve. Alternatively, the strain-hardening exponent can be obtained from equation (4) which can easily be solved with a non-linear iterative solver. This expression is derived in [8] by solving the instability point and converting true stress to engineering stress.

$$\frac{\sigma_{TS}}{\sigma_{YS}} = \frac{\left(\frac{n}{\epsilon_{YS}}\right)^n}{\exp(n)} \quad (4)$$

This study is limited to one material representative of most unirradiated RPVS. It has a hardening exponents $n=0.1$, a Young modulus $E=207$ GPa, a Poisson ratio $\nu=0.3$ and a yield stress such that $E/\sigma_{YS}=500$.

As most of valid fracture toughness tests on PCCv specimens do not show any ductile crack growth, the modelling of ductile crack growth by a complex node release technique is not necessary.

The first strategy is to use meshes containing 20-node isoparametric hexahedral elements with reduced Gauss integration. As no convergence was obtained for fine meshes, 8-node isoparametric hexahedral elements without reduced Gauss integration were also used.

Because of large geometry changes, the modified updated Lagrangian [9] procedure is used to account for large strains and displacements. To avoid large mesh deformation and overlapping at the crack tip, an initial blunted mesh is used. The initial crack tip radius is $10\ \mu\text{m}$. For the coarsest mesh, the dimension of the smallest element located at the crack tip is typically one third of the initial crack tip radius.

The specimen dimensions are standard: $10 \times 10 \times 55$ mm. As ASTM E1921-97, recommends a crack length to width ratio between 0.45 and 0.55, $a/W=0.5$ is selected for the present study. To reduce the computer time, only one fourth of the PCCv geometry was simulated (see Figure 1). Symmetry conditions were imposed to the planes defined by the equations $y=0$ and $z=5$. For the side-grooved geometry the thickness reduction is 20%, the notch angle 45° and the notch radius 0.5 mm in accordance with ASTM E1921-97. The side-grooved mesh was obtained by modifying the non side-grooved mesh. The nodes for which $y < y_{sg}$ are translated in the z direction, where $2y_{sg}$ is the side-groove width given by:

$$y_{sg} = \tan(\alpha/2) \left(d + r \left(\frac{1}{\sin(\alpha/2)} - 1 \right) \right) \quad (5)$$

where α is the notch angle, r the notch radius and d the notch depth.

For $z=0$ the nodes are translated to reproduce the notch shape. For $z \neq 0$, the translation vector reduces linearly from $z=0$ to $z=5$. The machined notch for precracking and for clip gauge attachment are not modelled as it will not affect the results.

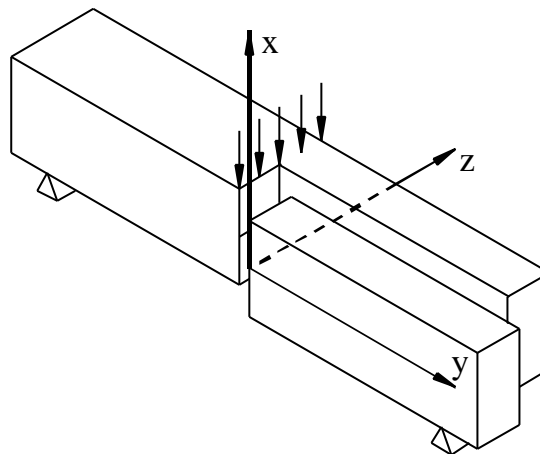


Figure 1 PCCv in 3PB loading. Only one fourth of the geometry is simulated.

Load application and support can be considered as contact conditions between the surface of different objects: the punch, the specimen and the roller. The introduction of these conditions in a finite element model is rather complex and introduces additional highly non-linear equations.

To simplify the problem, the support was initially simulated by fixing the displacement in the \bar{X} direction on the nodes located on the support line and the load was simulated by applying a displacement in the $-\bar{X}$ direction on the nodes located on the load line. The results on meshes of increasing refinement show that the model was too simplified and introduces local abnormal deformation near the load line and the support line.

In the final approach, thin elastic pentahedrons with the same Young modulus and Poisson ratio as the specimens are used to improve the load distribution on the contact areas (see Figure 2). The support is simulated by fixing the displacement in the \bar{X} direction on the nodes located on the edge of the pentahedron just above the support line and the load was simulated by applying a displacement in the $-\bar{X}$ direction on the nodes located at the edge of the pentahedron just below the load line.

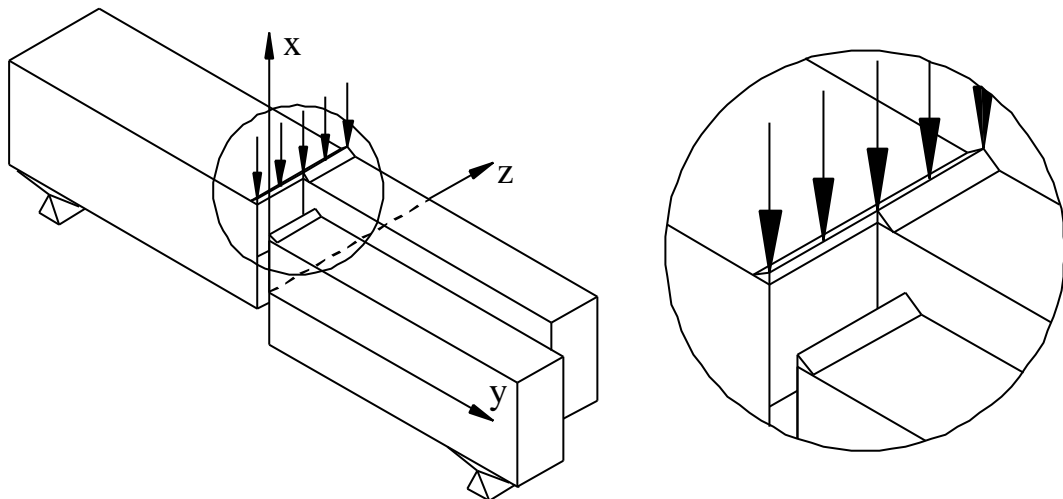


Figure 2 Simulated contact conditions for a PCCv loaded in 3PB. Pentahedrons have the following dimensions a thickness of 0.5 mm and a width of respectively 1.5 mm and 6 mm.

To model the geometry, it is simple to use a regular mesh, which is straightforward to generate. However, this would require a very long computer time for a given accuracy. The preferred strategy is to use a fine meshing in deformed regions and a coarse mesh in regions, which are less deformed. To check the accuracy of the obtained solution, calculations with different mesh density are compared. The adequate element size is obtained when the solution does not depend on the mesh size. Examples of meshing of PCCv without side-groove are given in Figure 3. Figure 4 shows an example of a mesh with side-groove. Table 1 shows the size of the problem.

Mesh	# elements	# nodes	
		linear (8 nodes)	quadratic (20 nodes)
M1	121	218	758
M2	968	1310	4869
M3	3267	3988	15193
M4	7744	8963	
M5	15125	16946	

Table 1 Size of the problem in term of number of elements and number of nodes.

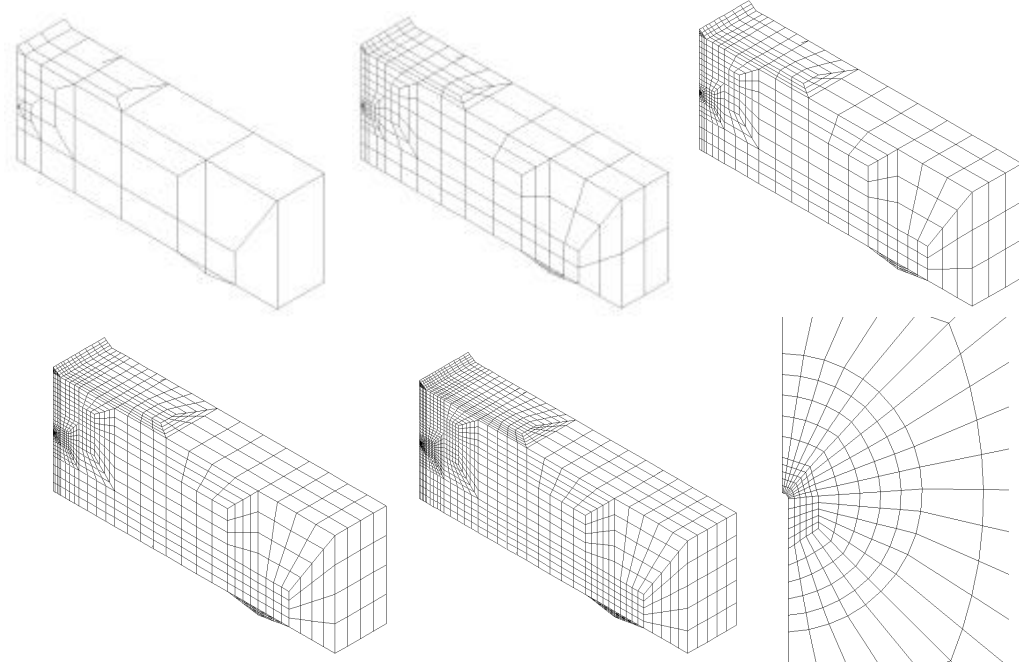


Figure 3 Meshing of PCCv without side-groove with different element density.

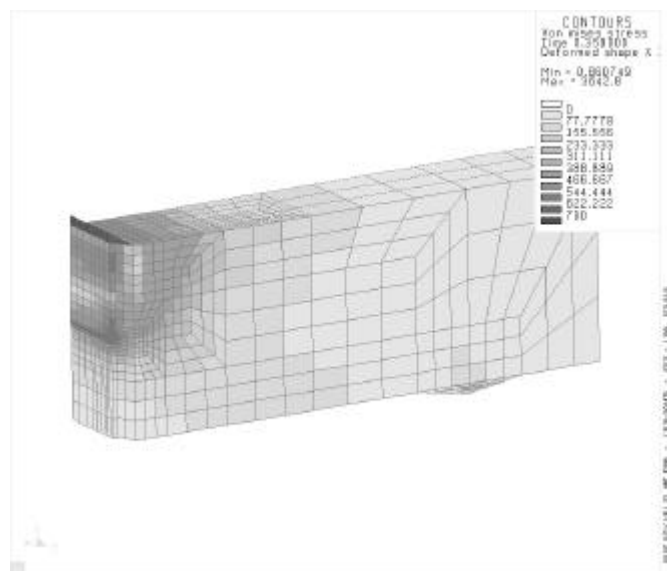


Figure 4 Side-grooved specimen loaded in 3-point bending. The radius of the side-groove notch is 0.5 mm.

The used finite element code, SYSWORLD, is a standard commercial code developed by the ESI group [9]. The algorithm used for the matrix inversion uses an iterative method to

decrease the size of the required RAM memory. The resolution of non-linear equation is performed using the BFGS algorithm. The number of load increments is typically 50.

The machine used for this project is a SUN Ultra 1 model 170E equipped with a Creator 3D graphic card. This machine has a single processor, which operates at 167 MHz. The initial amount of RAM was 64 MB and was successively extended to 128 MB and 1024 MB. The memory limits the size of the matrix that can be loaded. The disk space of 2 GB was also insufficient and two disks of 18.1 GB were added. The central process unit (CPU) time per load increment is 2400 sec for the mesh M5 with 8 nodes element and 3600 sec for mesh M3 with 8 nodes element. The complete resolution takes more time as the CPU time is always lower than the elapsed time and the pre- and post-processing is not included.

3 Finite element results

To ensure that results are independent of the mesh size, the load versus crack mouth opening displacement (CMOD) is given in Figure 5. The initial crack mouth opening or gauge length is taken equal to 5 mm. Figure 5 shows that results are not converged yet, from a global point of view, for mesh M1D1, M2D1 and M1D2. It means that 4000 well-distributed nodes are needed to converge independently of the element type (8-nodes or 20-nodes).

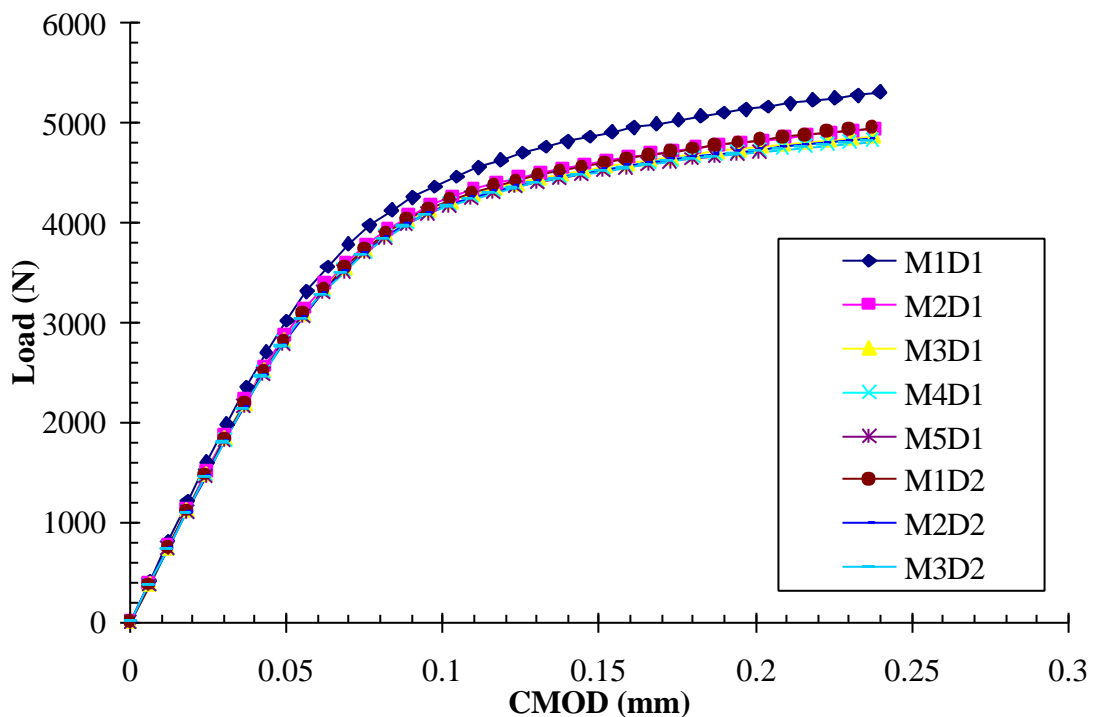


Figure 5 Effect of mesh size and element type on the overall behaviour. D1 and D2 relate to 8-nodes and 20-nodes element respectively.

For PCCv specimens, ASTM E1921-97 gives different possibilities to evaluate the fracture toughness from the load versus displacement record. The different possibilities are now assessed and compared to the direct evaluation of the J-integral.

The J-integral for a PCCv is evaluated as [1]:

$$J = \frac{K_e^2}{E} + J_p \quad (6)$$

where:

$$K_e = \frac{PS}{(BB_N)^{1/2} W^{3/2}} f(a_0/W) \quad (7)$$

$$f(a_0/W) = \frac{3(a_0/W)^{1/2}}{2(1+2a_0/W)} \frac{1.99 - (a_0/W)(1-a_0/W)[2.15 - 3.93(a_0/W) + 2.7(a_0/W)^2]}{(1-a_0/W)^{3/2}} \quad (8)$$

where P is the load, S the span, a_0 the initial crack length, W the specimen width, B the specimen thickness and B_N the specimen net thickness.

The standard method to evaluate the plastic component of the J-integral is based on the measure of the load line displacement where extra displacements due to the elastic compliance of the fixturing are subtracted (see ASTM E1921-97 §6.5.1). The standard proposes:

$$J_p = \frac{\eta A_p}{B_N b_0} \quad \text{with } \eta=1.9 \quad (9)$$

where b_0 is the initial ligament length.

A_p is the plastic area under the load (P) versus displacement curve given by:

$$A_p = A - 1/2 C_0 P \quad (10)$$

where A is the area under the load versus displacement curve and C_0 the reciprocal of the initial elastic slope.

It should be mentioned that the elastic compliance of the fixture generally displays a non-linear behaviour and hysteresis. These are mainly due to contact surfaces such as specimen-punch, specimen-roller, roller-three point bend support. Therefore, ASTM E1921-97 allows in §6.5.2 two alternative methods based on the crack-mouth opening displacement. The first method uses a η -factor developed for this position [7] and the second method uses a load-point displacement inferred from the CMOD [10].

The η -factor calculated from 3-D finite element analysis by Nevalainen and Dodds [7] are given in Table 2. A tabulated η -factor is not very practical to be used in a standard. Therefore, they refer to the work of Kirk and Dodds [11] where 2-D plane strain calculations were used to establish a closed form of the η -factor:

$$\eta_{\text{CMOD}} = 3.785 - 3.101(a_0/W) + 2.018(a_0/W)^2 \quad S=4W \quad (11)$$

In both cases calculations were performed with $S=4W$. A generalisation of equation (11) is proposed in [11] and applied to miniature specimen for which a larger span than $4W$ had to be used. The generalised equation is:

$$\eta_{\text{CMOD}} = \frac{S}{4W} (3.785 - 3.101(a_0/W) + 2.018(a_0/W)^2) \quad (12)$$

It should be noted that in both references [7] and [11], the elastic component of J is not calculated as in equation (6) proposed by the ASTM, but as:

$$J = \frac{(1-\nu^2)K_e^2}{E} + J_p \quad (13)$$

Considering the values in Table 2 as the reference, equation (11) can lead to 10 % over-estimation of the plastic part of the J-integral for SG, $a/W=0.5$ and $1/n=10$.

a/W	W/B	1/n	$\eta_{\text{CMOD}}[7]$	$\eta_{\text{CMOD}}[11]$
0.1	4	5	3.59	3.495
0.1	4	10	3.45	3.495
0.1	4	20	3.43	3.495
0.1	2	5	3.66	3.495
0.1	2	10	3.53	3.495
0.1	2 (SG)	10	3.34	3.495
0.1	2	20	3.51	3.495
0.1	1	5	3.55	3.495
0.1	1	10	3.41	3.495
0.1	1	20	3.43	3.495
0.5	4	5	2.65	2.739
0.5	4	10	2.60	2.739
0.5	4	20	2.53	2.739
0.5	2	5	2.64	2.739
0.5	2	10	2.59	2.739
0.5	2 (SG)	10	2.48	2.739
0.5	2	20	2.57	2.739
0.5	1	5	2.70	2.739
0.5	1	10	2.67	2.739
0.5	1	20	2.66	2.739

Table 2 Tabulated values of the h -factor for the evaluation of J_p from the plastic energy under the load versus CMOD. SG refers to the side-grooved geometry.

The second alternative is to infer the load-point displacement from the CMOD. The inferred load-point displacement is then used in equation (9). ASTM E1921-97 refers to the work of Underwood et al. [10] where different expressions are discussed. The proposed equation established for $S=4W$ and for $0 \leq a_0/W \leq 1$ is:

$$\frac{\delta}{\text{CMOD}} = \frac{1}{1.384(a_0/W) - 1.497(a_0/W)^2 + 2.339(a_0/W)^3 - 1.226(a_0/W)^4} \quad (14)$$

with δ , the load point displacement.

As the load point displacement increases with the span for a given CMOD, a generalisation for $S \neq 4W$ is proposed:

$$\frac{\delta}{\text{CMOD}} = \frac{S/(4W)}{1.384(a_0/W) - 1.497(a_0/W)^2 + 2.339(a_0/W)^3 - 1.226(a_0/W)^4} \quad (15)$$

In most of the work performed at SCK•CEN before 1999, the load line displacement is inferred from the CMOD using a formula based on geometrical considerations and a plastic rotational factor, r_p [10].

$$\frac{\delta}{\text{CMOD}} = \frac{S/(4W)}{r_p(1 - a_0/W) + (a_0/W) \cos \left[a \tan \left(\frac{\text{CMOD}/2}{r_p(W - a_0) + a_0} \right) \right]} \quad (16)$$

The plastic rotational factor, r_p , is taken equal to 0.44 for $0.45 = a_0/W = 0.55$ [10, 16]. The plastic rotational factor, r_p , is a useful concept that can also be used to measure the crack tip opening displacement, CTOD, or to correct clip gauge displacements when razor blades are used [16]. The accuracy of this equation is poor in the elastic regime but allows an accurate determination of the plastic part, which is of interest to determine the plastic contribution of the J-integral.

It should be noted that for small and large deformation the previous equation reduces to:

$$\frac{\delta}{\text{CMOD}} = \frac{S/(4W)}{a_0/W + r_p(1 - a_0/W)} \quad (17)$$

For a PCCv specimen loaded up to $130 \text{ MPa}\sqrt{\text{m}}$ the difference is negligible (about 0.02%). Therefore equation (16) and (17) should be considered as strictly equivalent in the domain investigated here.

The previous evaluations of the J-integral from the load versus displacement record can be compared to a direct evaluation of the J-integral from the finite element calculations. For a 3-D configuration, the loading of the specimen is measured through the average J-integral along the crack front, which is defined as:

$$J = \frac{1}{L} \lim_{\epsilon \rightarrow 0} \int_{A_\epsilon} (W n_x - \sigma_{ij} \partial_x u_i n_j) dA_\epsilon \quad (18)$$

where x is the direction of crack propagation, L the crack length, A_ϵ a tubular surface around the crack front, W the energy density, n the external normal to A_ϵ , σ the stress tensor and u the displacement vector.

The J-integral as expressed in equation (18) cannot be directly and accurately evaluated from the finite element results, as just ahead of the crack tip large stresses and strain gradients are expected. Therefore, the J-integral is transformed into an equivalent domain integral (EDI) [8, 12]. In absence of thermal load, volumic forces and stresses or displacements applied to the crack lips, the EDI reduces to:

$$J = \frac{-1}{L} \int_V (W \partial_x q - \sigma_{ij} \partial_x u_i \partial_j q) dV \quad (19)$$

where V is a tubular volume around the crack front, q any continuous function with a value of one at the crack tip and zero at the external border of V . In this work, q is chosen equal to a quadratic function of the radial coordinate with a slope of zero at the crack tip front and at the external border of V [14].

From a theoretical point of view, the J-integral obtained from the EDI method is independent of the size of the tubular volume under different hypotheses [14]: small strain, proportional loading with no partial unloading and existence of a potential function with a unique relationship between stress and strain.

The path dependence of the J-integral is assessed in Figure 6. One can see that the J-integral becomes path independent for a sufficiently large path-radius. The path independence is better for low load and when a small strain model is used. In this work, the more realistic finite strain model is used and the J-integral will be evaluated with the EDI method using a cylindrical volume with the largest radius (the radius is 5 mm for a PCCv with $a/W=0.5$).

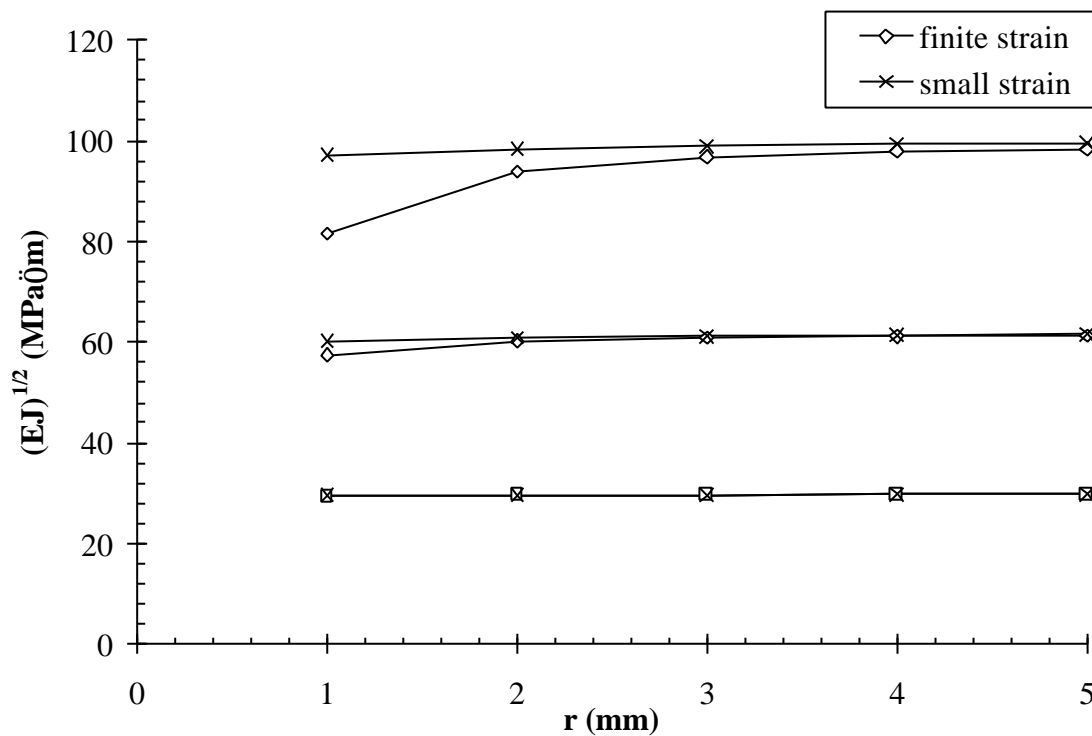


Figure 6 J-integral calculated using the EDI method with cylindrical volume of different radius. Figure obtained with mesh M4D1.

Taking the J-integral calculated by the EDI method as the reference value, the different methods are compared in Figure 7 and Figure 8 for respectively non side-grooved and side-grooved PCCv geometry. The different methods are nicknamed:

- LPD for equation (6) combined with equation (9)
- CMOD for equation (6) combined with equation (12)
- LPD1(CMOD) for equation (6) combined with equations (9) and (15)
- LPD2(CMOD) for equation (6) combined with equations (9) and (16)

Figure 7 and Figure 8 show that all methods have an acceptable accuracy of 5% on K_J except when the LLD is inferred from the CMOD using the relation proposed by Underwood et al. [10]. This 5% error on K_J contributes to an error of 3 °C only on the reference temperature, T_0 .

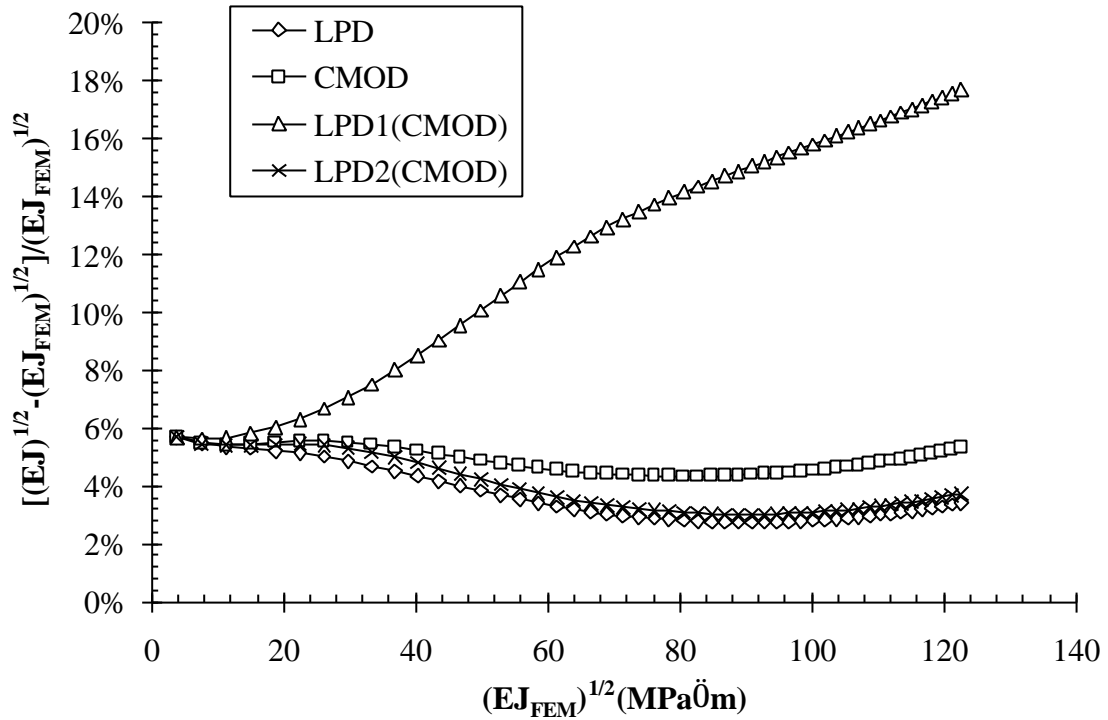


Figure 7 Comparison of J obtained from the load versus displacement curves to the J -integral calculated from finite element calculations for a non side-grooved PCCv geometry.

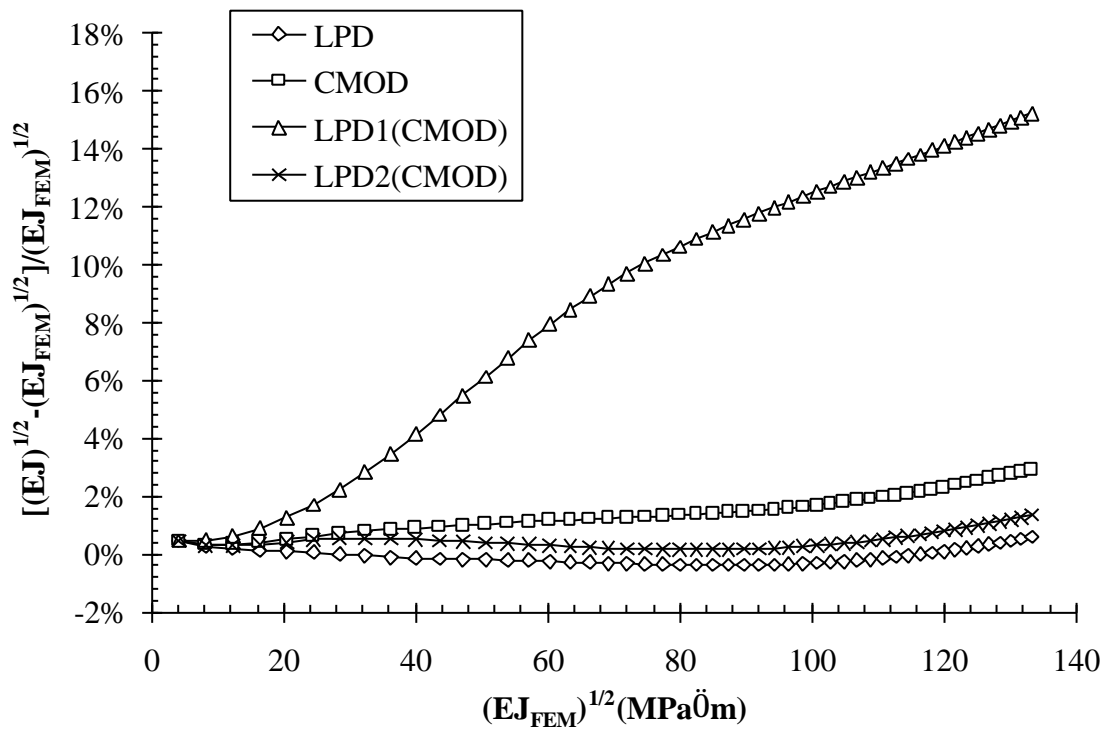


Figure 8 Comparison of J obtained from the load versus displacement curves to the J -integral calculated from finite element calculations for a side-grooved PCCv geometry.

4 Discussion

In [7], a meshing with 7700 8-nodes elements and a total of 9300 nodes was used. This meshing corresponds to M4 with 8-nodes elements, which is demonstrated to give converging results. In [7], about 60 seconds CPU-time is needed to solve a load increment on a Cray-90 supercomputer using a single vectorised processor. In our case, a time step was solved in about 1188 seconds CPU time. The gain of a factor 20 in speed can be attributed to the supercomputer and to the tuning of the code for a vectorised processor.

According to ASTM E1921-97, the relation between the stress intensity factor K and the J integral is:

$$J = \frac{K_e^2}{E} + J_p \quad (20)$$

However in most of the literature the plane strain Young modulus is used:

$$J = \frac{(1-\nu^2)K_e^2}{E} + J_p \quad (21)$$

The maximum difference between the two formulations is 5% on the stress intensity factor, which results in about 3°C on the reference temperature.

From a theoretical point of view, the relation between the stress intensity factor K and the J -integral exists only in the elastic domain. The more general form is [12]:

$$J = \frac{1}{E^*} (K_I^2 + K_{II}^2) + \frac{1+\nu}{E} K_{III}^2 \quad (22)$$

which for mode I loading reduces to:

$$J = \frac{K_I^2}{E^*} \quad (23)$$

where the equivalent Young modulus E^* is:

$$E^* = E \left(\frac{1}{1-\nu^2} + \frac{\nu}{1+\nu} \varepsilon_r \right) \quad (24)$$

with

$$\varepsilon_r = \frac{\sigma_r - \nu}{1 - \nu(1 + 2\sigma_r)} \quad (25)$$

$$\varepsilon_r = \frac{\varepsilon_{33}}{\varepsilon_{11} + \varepsilon_{22}} \quad \text{and} \quad \sigma_r = \frac{\sigma_{33}}{\sigma_{11} + \sigma_{22}} \quad (26)$$

where stress and strain tensors are taken close to the crack tip in the local axis of the crack front.

Consequently:

$$E^* = \frac{E}{1-\nu^2} \quad \text{in plane strain} \quad (27)$$

$$E^* = E \quad \text{in plane stress} \quad (28)$$

In the elastic domain, the crack front of a PCCv specimen is in a plane strain configuration. The J-integral is thus related to the stress intensity factor through:

$$J = \frac{(1-\nu^2)K_e^2}{E} \quad (29)$$

When plasticity develops a term should be added. This term should vanish when no plasticity is observed. Therefore, the relation should have the following form:

$$J = \frac{(1-\nu^2)K_e^2}{E} + J_p \quad (30)$$

It may be argued that when plasticity develops the crack tip condition can move from a plane strain to plane stress condition. However, the stress intensity factor loses its significance when plasticity develops. Equation (30) should only be seen as an empirical formula to obtain the J-integral as defined by equation (18). For convenience an elastic-plastic equivalent stress intensity factor K_J can be defined such that it reduces to the stress intensity factor in elastic conditions:

$$K_J = \sqrt{\frac{EJ}{1-\nu^2}} \quad (31)$$

In ASTM E1921-97, the experimental determination of K_J is taken based on $K_J = \sqrt{EJ}$, which allows a conservative estimate of the fracture toughness.

The result of our investigation is compared to literature in Table 3. In accordance with [7], η_{LLD} and η_{CMOD} are obtained by the slope of the linear fit imposing that an intercept equal 0 as illustrated in Figure 9. The maximum difference with the result of Nevalainen and Dodds [7] and Koppenhoefer and Dodds [15] is 6%. This difference should be considered as small as a 6% error on the J-integral corresponds to 3% on K_J and to 2 °C in terms of reference temperature T_0 .

		this work	[7]	[15]	ASTM E1921-97
f(a/W)	not SG	2.641	n.a.	n.a.	2.6625
	SG 20%	2.778	n.a.	n.a.	2.6625
η_{LLD}	not SG	1.816	1.86	1.9	1.9
	SG 20%	1.899	1.74 [‡]	2	1.9
η_{CMOD}	not SG	2.504	2.67	2.7	2.738
	SG 20%	2.594	2.48 [‡]	2.88 [‡]	2.738

Table 3 Comparison of the parameters used to calculate the stress intensity factor K and the J -integral. Calculation are done with a PCCv specimen with $a/W=5$, $n=0.1$ and $E/s_{YS}=500$.

[‡]Calculations were performed with $W/B=2$. No calculations were available in [7] with $W/B=1$. [‡]It was supposed that the value in [15] was not scaled by B_N .

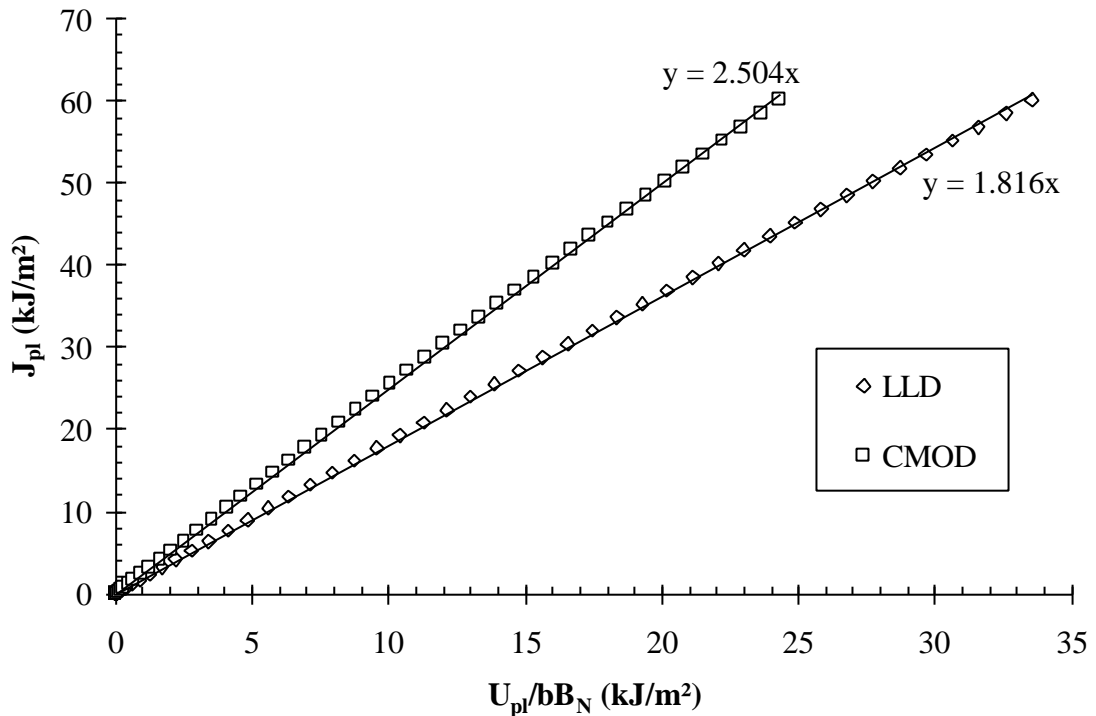


Figure 9 h_{LLD} and h_{CMOD} are obtained by the slope of the linear fit imposing the intercept equal 0.

As shown in Figure 7 and Figure 8, and contrary to equation (16) the relation to infer the LLD from the CMOD proposed by Underwood et al. [10] is inadequate to calculate the J integral. The reason for this discrepancy is discussed hereafter.

In the elastic regime, the LLD is obtained from the ratio between the load line compliance and the crack opening compliance [10]. An analytical relationship is proposed in [10] and generalised for S different than $4W$.

$$LLD_{el.} = \frac{S/(4W)}{g_1(a/W)} CMOD_{el.} \quad (32)$$

with

$$g_1(a/W) = 1.718(a/W) - 1.302(a/W)^2 + 1.039(a/W)^3 - 0.452(a/W)^4 \quad (33)$$

In the plastic regime a similar equation is obtained:

$$LLD_{pl.} = \frac{S/(4W)}{g_2(a/W)} CMOD_{pl.} \quad (34)$$

with

$$g_2(a/W) = r_p + (1 - r_p)(a/W) \quad (35)$$

A general expression can be obtained by combining the previous equation:

$$LLD = \frac{S/(4W)}{g_1(a/W)} CMOD_{el.} + \frac{S/(4W)}{g_2(a/W)} CMOD_{pl.} \quad (36)$$

An error on g_1 will not affect the calculation of the plastic part of J. Therefore, taking g equal g_2 as in equation (17) is a good strategy.

It should be noted that g_2 can simply be obtained from the η -factor:

$$g_2(a/W) = \frac{\eta_{LLD}}{\eta_{CMOD, S=4W}} \quad (37)$$

The comparison of the g_1 and g_2 functions is given in Table 4 and Table 5. For the elastic part of g_1 , the finite element calculations are in good agreement with the analytical formulation. For the plastic part g_2 , all equations are within 5% except equation (15) which is clearly too small. The reason for this large discrepancy is attributed to the limit of applicability in which the equation was established. Although not clearly states, the equation only applies to high-strength steels where limited plasticity develop. The reason for this limited application range is now further investigated. In the paper of Underwood et al. [10], the LLD is split in a part due to the crack and a part due to elastic bending (no crack).

$$LLD_{NC} = \frac{P}{EB} \frac{S^3}{4W^3} \quad (38)$$

The elastic part due to bending is then expressed in terms of the CMOD through the compliance.

$$LLD_{NC} = \frac{CMOD}{C_{CMOD}} \frac{S^3}{EB 4W^3} \quad (39)$$

where C_{CMOD} is the CMOD compliance.

For an elastic plastic material, this is of course an error as the elastic part due to bending can only be a function of the elastic part of the CMOD. In fact, in this step there is the underlying hypothesis that the material is a high strength steel with limited plasticity.

It should be noted that the g_1 and g_2 coefficients obtained in this work lead to a relative error on the LLD lower than 0.6%.

		this work	eq. (33)
g_1	not SG	0.620	0.635
	SG 20%	0.627	0.635

Table 4 Comparison of g_1 for a PCCv specimen with $a/W=5$, $n=0.1$ and $E/s_{YS}=500$.

		this work	[7]	[15]	eq. (17)	eq. (15)	eq. (9) and (12)
g_2	not SG	0.725	0.697	0.704	0.72	0.534	0.694
	SG 20%	0.732	0.702 [‡]	0.694	0.72	0.534	0.694

Table 5 Comparison of g_2 for a PCCv specimen with $a/W=5$, $n=0.1$ and $E/s_{YS}=500$.

[‡]Calculations were performed with $W/B=2$. No calculation were available with $W/B=1$.

CONCLUSIONS

Three-dimensional finite element calculations performed on side-grooved and non side-grooved PCCv specimens for $a/W=0.5$ are presented in the present report.

The main deliverables of this investigation are:

- Three-dimensional calculations are time consuming and require efficient hardware and software.
- When an adequate mesh is used, at least 4000 nodes are required to be mesh-size independent.
- Although it can be improved, the different formulations proposed in the ASTM E1921-97 to calculate the J-integral are sufficiently accurate for its application. The maximum error on the reference temperature is 3 °C.
- Although the difference is small, it is demonstrated that the plane strain Young modulus should be used instead of the plane stress Young modulus.
- The formulation of Underwood et al. [10], Equation (15), to infer the LLD from the CMOD should only be used for high strength steel material for which plastic deformation is very limited.
- The results are in good agreement with finite element calculations performed by Nevalainen and Dodds [7] and Koppenhoefer and Dodds [15].

In further work the comparison with the one-inch thickness compact tension specimen will be performed in order to investigate the size effect and the loss of constraint.

ACKNOWLEDGEMENTS

I would like to thank the technical staff of SCK•CEN and particularly David De Maeyer for his valuable support for the optimised use of the workstation. The present work is partly financed by Tractebel Energy Engineering. Their support is kindly appreciated.

REFERENCES

- [1] ASTM E 1921-97 "Test method for the determination of reference temperature, T_0 , for ferritic steels in the transition range", Annual book of ASTM standards" Section 3 Vol. 03.02 Metals Test Methods and Analytical Procedures, Printed in Easton, MD, USA, 1998
- [2] E. van Walle "Reconstitution: where do we stand ?", Effects of irradiation on materials: 17th international symposium, ASTM STP 1270, D.S. Gelles, R.K. Nansdstad, A.S. Kumar and E.A. Little, Eds., American Society for Testing Materials, 415-441, 1996
- [3] E. Lucon and M. Scibetta "Comparison between precracked Charpy-V and C(T) specimens for T_0 determination of the JSPS RPV steel", report R-3378 Rev. 1, SCK•CEN, Mol, Belgium, January 2000
- [4] R. Chaouadi, M. Scibetta, E. van Walle and R. Gerard "On the use of the master curve based on the precracked charpy specimen", Pressure Vessel and Piping Symposium, "Fracture, Fatigue and Weld Residual Stress ", Vol 393, pp. 35 -46, 1999
- [5] Lee Bong-Sang, Yang Won-Jon, Kim Joo-Hag, Hong Jun-Hwa and Lee Byong-Whi "Determination of the fracture toughness transition temperature, T_0 , of the IAEA and Korean Reference Materials, JRQ, JFL, KFY5", presented at the RCM of the CRP on "Assuring Structural Integrity of Reactor Pressure Vessels", Vienna Austria, November 17-19, 1999
- [6] Dodds R.H., Carpenter W.C. and Sorem W.A. "Numerical evaluation of a 3-D J-integral and comparison with experimental results for a 3-point bend specimen", Engineering Fracture Mechanics Vol. 29, No. 3, pp. 275-285, 1988 Nevalainen M. and
- [7] Nevalainen M. and Dodds R.H.Jr. "Numerical investigation of 3-D Constraint Effects on Brittle Fracture in SE(B) and C(T) Specimens", Report UILU-ENG-95-2001, Department of civil engineering, university of illinois at Urbana-Champaign Urbana, Illinois, February 1995
- [8] Scibetta M. "Contribution to the Evaluation of the Circumferentially-Cracked Round Bar for Fracture Toughness Determination of Reactor Pressure Vessel Steels", Dissertation for the Degree of Doctor in Applied Sciences, Université de Liège, March 1999.
- [9] ESI Group, SYSTUS+ 2.0, Analysis Reference Manual, 1998

- [10] Underwood J.H., Troiano E.J. and Abbott R.T. "Simpler J_c Test and Data Analysis Procedures for High-Strength Steels", Fracture mechanics: "Twenty-Fourth Volume, ASME STP 1207, John D. Landes, Donald E. McCabe and J.A.M. Boulet, Eds., American Society for Testing and Materials, Philadelphia, pp. 410-421, 1994
- [11] Kirk M.T. and Dodds R.H.Jr. "J and CTOD Estimation Equations for Shallow Cracks in Single Edge Notch Bend Specimens", Journal of Testing and Evaluation, JTEVA, Vol. 21, No. 4, pp. 228-238, July 1993
- [12] Nikishkov G.P. and Alturi S.N. "Calculation of fracture mechanics parameters for an arbitrary three-dimensional crack, by the 'equivalent domain integral' method", Int. Journal for numerical methods in engineering, Vol. 24, pp. 1801-1821, 1987
- [13] Lucon E. and Scibetta M." Fracture toughness measurements in the transition regime using miniature PCCv and CRB specimens", SCK•CEN, Mol, Belgium, report R-3400, February 2000
- [14] Scibetta M. "Fracture toughness evaluation of circumferentially-cracked round bars", report BLG-716, SCK-CEN Mol, Belgium, May 1996
- [15] Koppenhoefer K. C. and Dodds R.H. "Loading rate effects on cleavage fracture of pre-cracked CVN specimens: 3-D studies", ", Engineering Fracture Mechanics Vol. 58, No. 3, pp. 249-270, 1997
- [16] A.S.T.M. E1820-99, "Standard Test Method for Measurement of Fracture Toughness", Annual book of ASTM Standards, January, 1999